

An Improved Random Matrix Prediction Model for Manoeuvring Extended Targets

Nathan J. Bartlett, Chris Renton, Adrian G. Wills

Abstract—This paper proposes an improved prediction update for extended target tracking with the random matrix model. A key innovation is to employ a generalised non-central inverse Wishart distribution to model the state transition density of the target extent; resulting in a prediction update that accounts for kinematic state dependent transformations. Moreover, the proposed prediction update offers an additional tuning parameter c.f. previous works, requires only a single Kullback-Leibler divergence minimisation, and improves overall target tracking performance when compared to state-of-the-art alternatives.

Index Terms—Extended target tracking, random matrix model, non-central inverse Wishart, Kullback-Leibler divergence.

I. INTRODUCTION

TARGET tracking is an important practical problem that has received significant research attention since the pioneering works of [1]. Due to an increase in sensor resolution capabilities, it is now commonplace for multiple measurements to be generated for each target per time-step; e.g., modern radar can produce several range measurements for a single target. One approach to handle the generation of multiple measurements is to employ extended-target models, where, in addition to estimating the kinematic state variables, the spatial extent of the target is estimated from available data. In recognition of the utility of extended targets, several models have been proposed over the past decade, see e.g., [2]–[10].

One of the most popular extended-target models, referred to as the *random matrix model*, was first proposed in the works of Koch [10]; and defines the extended target state as the combination of a kinematic state vector and an extent matrix. The extent matrix is assumed to be symmetric positive definite, which in turn enables for the target extent to be represented by an ellipsoid [11]. The kinematic state vector is modelled as a Gaussian distributed random variable, whilst the extent matrix is modelled as an inverse Wishart distributed random variable. Following a Bayesian methodology, the prediction density of each random variable is assumed to belong to the same distribution class of its respective posterior, enabling for the parameters of each density to be updated recursively; consisting of a prediction and a correction stage.

In the early work of Koch and Feldmann *et al.* [10], [11], the prediction update of the extent matrix was based upon a simple heuristic that artificially increased the covariance whilst preserving the expected value. Koch additionally proposed the use of a Wishart state transition density [10], which was later generalised within [12], [13] to handle temporal

evolutions of the target extent. However, even for evolutions independent of the kinematic state, a second-order moment matching technique or Kullback-Leibler divergence minimisation is required to approximate the resulting Generalised Beta Type-II prediction density as an inverse Wishart distribution; instigating information loss in regard to the target extent [14]. To resolve this issue, Bartlett *et al.* [14] proposed the use of a non-central inverse Wishart state transition density, which was shown to produce an inverse Wishart prediction distribution directly and significantly improve target extent estimation.

Contributions: The key contribution of this paper is the generalisation of the non-central inverse Wishart state transition density to account for kinematic state dependent evolutions of the target extent. This generalisation is motivated by the works of [13], whom, to the best of the authors' knowledge, were the first to propose a prediction update to handle kinematic state dependent evolutions of the target extent. The main difference here is that by building upon [14], our proposed prediction update requires only a *single* Kullback-Leibler divergence minimisation, and offers an additional tuning parameter to model uncertainties in target shape more effectively.

The remainder of the paper is organised as follows. In Section II, we provide an overview of the random matrix model and the prediction updates of [10]–[14]. The problem formulation is presented in Section III, and the proposed prediction update is given in Section IV. Simulated results comparing the proposed prediction update against state-of-the-art alternatives are presented in Section V. Concluding remarks are given in Section VI. Notation and distributions are summarised in Table I.

II. THE RANDOM MATRIX MODEL

The random matrix model can be accredited to the works of Koch and Feldmann *et al.* [10], [11]. The model has been used in an wide array of extended-target tracking applications over the last decade, including aircraft tracking with ground radar, pedestrian tracking with laser range sensors, and surface vessel tracking with marine X-band radar; see e.g., [15]–[22].

The random matrix model defines the extended target state $\xi_k \triangleq (\mathbf{x}_k, X_k)$ at time t_k as the combination of a kinematic state vector $\mathbf{x}_k \in \mathbb{R}^{n_x}$ and an extent matrix $X_k \in \mathbb{S}_{++}^d$. The kinematic state vector consists of states related to the motion of the target centre, whilst the extent matrix models the target extent as a d -dimensional ellipsoid [14]. Thus, the region of space $\mathcal{Y} \subseteq \mathbb{R}^d$ occupied by the extended target at time t_k can be described by the following set:

$$\mathcal{Y} \triangleq \{\mathbf{y} \in \mathbb{R}^d : (\mathbf{y} - H_k \mathbf{x}_k)^T X_k^{-1} (\mathbf{y} - H_k \mathbf{x}_k) \leq 1\}, \quad (1)$$

All authors are within the Faculty of Engineering and Built Environment, The University of Newcastle, Australia.

Corresponding author e-mail: nathan.bartlett@uon.edu.au

where H_k is a matrix that transforms the kinematic state vector to a target position. In the conditional random matrix model, the kinematic state can only consist of the target position and time derivatives such as velocity and acceleration [10]. In the factorised random matrix model—which shall be utilised in this paper—the kinematic state can also include non-linear kinematics such as turn-rate and heading [11]. The measurements $\mathbf{z}_k^r \in \mathbf{Z}_k$ at time t_k are assumed to be multivariate Gaussian distributed with covariance related to the extent matrix

$$p(\mathbf{Z}_k | \xi_k) = \prod_{r=1}^{m_k} \mathcal{N}(\mathbf{z}_k^r | H_k \mathbf{x}_k, \lambda X_k + R_k), \quad (2)$$

where R_k is the sensor noise covariance, and λ is the scaling factor to the spread contribution of the target extent [11].

In situations where the sensor noise covariance R_k has negligible impact upon the spatial distribution of the measurements¹, Koch showed that an inverse Wishart probability density function, or pdf, is a conjugate prior to (2). Hence, the factorised random matrix model defines the posterior of the extended target state ξ_k as the product of a Gaussian kinematic state density and an inverse Wishart extent matrix density [11]. More specifically, the posterior distribution is approximated as

$$p(\xi_k | \mathbf{Z}^k) \approx p(\mathbf{x}_k | \mathbf{Z}^k) p(X_k | \mathbf{Z}^k), \quad (3a)$$

where $\mathbf{Z}^k = \{\mathbf{Z}_1, \dots, \mathbf{Z}_k\}$ is the set of all measurement sets up to and including time t_k , and

$$p(\mathbf{x}_k | \mathbf{Z}^k) = \mathcal{N}(\mathbf{x}_k | \mathbf{m}_{k|k}, P_{k|k}), \quad (3b)$$

$$p(X_k | \mathbf{Z}^k) = \mathcal{IW}_d(X_k | \nu_{k|k}, V_{k|k}). \quad (3c)$$

In Bayesian estimation, it is often desired for the prediction density to belong to the same distribution class as the posterior. By satisfying this condition, the parameters of the chosen class of distribution can be updated in Bayesian recursion rather than the entire distribution itself. Therefore, to obtain a computationally efficient filter, we want to ensure that the prediction density is of the same functional form as the posterior (3); i.e., we want

$$p(\xi_{k+1} | \mathbf{Z}^k) \approx p(\mathbf{x}_{k+1} | \mathbf{Z}^k) p(X_{k+1} | \mathbf{Z}^k), \quad (4a)$$

where

$$p(\mathbf{x}_{k+1} | \mathbf{Z}^k) = \mathcal{N}(\mathbf{x}_{k+1} | \mathbf{m}_{k+1|k}, P_{k+1|k}), \quad (4b)$$

$$p(X_{k+1} | \mathbf{Z}^k) = \mathcal{IW}_d(X_{k+1} | \nu_{k+1|k}, V_{k+1|k}). \quad (4c)$$

Assuming this condition is satisfied, the prediction update corresponds to obtaining the parameters $\{\mathbf{m}_{k+1|k}, P_{k+1|k}\}$, and $\{\nu_{k+1|k}, V_{k+1|k}\}$ of the predicted Gaussian kinematic state vector density (4b) and the predicted inverse Wishart extent matrix density (4c) respectively.

In the early work of Feldmann *et al.* [11], an extended Kalman filter prediction is utilised to obtain the parameters of the predicted kinematic state vector density (4b). Moreover,

¹ $R_k \approx 0_d$ to prove conjugacy [10]. In scenarios where this approximation is invalid, additional heuristics are required to obtain a closed-form correction; see [11] for further details.

TABLE I: Notation

- I_n is a $n \times n$ identity matrix, and 0_m is a $m \times m$ zero matrix.
- \mathbb{R}^n is the set of real column vectors of length n , $\mathbb{R}^{m \times n}$ is the set of real $m \times n$ matrices, \mathbb{S}_{++}^n is the set of symmetric positive definite $n \times n$ matrices, \mathbb{S}_+^n is the set of symmetric positive semi-definite $n \times n$ matrices, \mathbb{N} is the set of natural numbers, $\mathbb{SL}(n, \mathbb{R})$ is the special linear group of $n \times n$ matrices with determinant equal to one, and $\mathbb{O}^{m \times n}$ is the set of $m \times n$ semi-orthogonal matrices with $m \leq n$.
- $\mathcal{N}(\mathbf{x} | \mathbf{m}, P)$ denotes a multivariate Gaussian pdf defined over the vector $\mathbf{x} \in \mathbb{R}^n$, with expectation $\mathbf{m} \in \mathbb{R}^n$ and covariance matrix $P \in \mathbb{S}_{++}^n$,

$$\mathcal{N}(\mathbf{x} | \mathbf{m}, P) = \frac{\exp(-\frac{1}{2}(\mathbf{x} - \mathbf{m})^T P^{-1}(\mathbf{x} - \mathbf{m}))}{(2\pi)^{\frac{n}{2}} |P|^{\frac{1}{2}}},$$

where $|\cdot|$ denotes the matrix determinant.

- $\mathcal{IW}_d(X | \nu, V)$ denotes an inverse Wishart pdf defined over the matrix $X \in \mathbb{S}_{++}^d$ with scalar degrees of freedom $\nu > 2d$ and parameter matrix $V \in \mathbb{S}_{++}^d$ [23, Definition 3.4.1],

$$\mathcal{IW}_d(X | \nu, V) = \frac{\text{etr}(-\frac{1}{2} V X^{-1}) |V|^{\frac{\nu-d-1}{2}}}{2^{\frac{d(\nu-d-1)}{2}} \Gamma_d(\frac{\nu-d-1}{2}) |X|^{\frac{\nu}{2}}},$$

where $\text{etr}(\cdot) = \exp(\text{Tr}(\cdot))$ represents the exponential of the matrix trace, and $\Gamma_d(\cdot)$ is the multivariate Gamma function which can be expressed as a product of ordinary gamma functions $\Gamma(\cdot)$ [23, Theorem 1.4.1]. The expectation of X is $V/(\nu - 2d - 2)$ [23, Theorem 3.4.3].

- $\mathcal{W}_d(X | w, W)$ denotes a Wishart pdf defined over the matrix $X \in \mathbb{S}_{++}^d$ with scalar degrees of freedom $w > d - 1$ and parameter matrix $W \in \mathbb{S}_{++}^d$ [23, Definition 3.2.1],

$$\mathcal{W}_d(X | w, W) = \frac{\text{etr}(-\frac{1}{2} X W^{-1}) |X|^{\frac{w-d-1}{2}}}{2^{\frac{wd}{2}} \Gamma_d(\frac{w}{2}) |W|^{\frac{w}{2}}}.$$

- $\mathcal{GB}_d^{II}(X | a, b, \Omega, \Psi)$ denotes a Generalised Beta Type II pdf defined over the matrix $X \in \mathbb{S}_{++}^d$ with scalar parameters $a, b > \frac{d-1}{2}$, and matrices $\Omega \in \mathbb{S}_{++}^d$, $\Psi \in \mathbb{S}_{++}^d$ [23, Definition 5.2.4],

$$\mathcal{GB}_d^{II}(X | a, b, \Omega, \Psi) = \frac{|X - \Psi|^{a-\frac{d+1}{2}} |X + \Omega|^{-(a+b)}}{\beta_d(a, b) |\Omega + \Psi|^{-b}},$$

where $\beta_d(a, b)$ is the multivariate beta function, and can be expressed in terms of the multivariate Gamma function $\Gamma_d(\cdot)$ [23, Theorem 1.4.2].

- $\mathcal{IW}_d^{nc}(X | \nu, \Sigma, \Sigma\Theta)$ denotes a non-central inverse Wishart pdf defined over the matrix $X \in \mathbb{S}_{++}^d$ with scalar degrees of freedom $\nu > 2d$, parameter matrix $\Sigma \in \mathbb{S}_{++}^d$, and non-centrality parameter matrix $\Theta \in \mathbb{S}_{++}^d$ [23, Definition 3.5.2],

$$\mathcal{IW}_d^{nc}(X | \nu, \Sigma, \Sigma\Theta) = \frac{\mathcal{IW}_d(X | \nu, \Sigma) \text{etr}(-\frac{1}{2} \Sigma\Theta)}{{}_0F_1(\frac{\nu-d-1}{2}; \frac{1}{4} \Sigma\Theta \Sigma^{-1})^{-1}},$$

where ${}_0F_1(\cdot)$ is the hypergeometric function of matrix argument [23, Theorem 1.6.4]. When $\Theta = 0_{d,d}$ the distribution reduces to the inverse Wishart distribution.

the parameters of the predicted extent matrix density (4c) are obtained via a simple heuristic that preserves the expected value whilst artificially increasing the covariance—resembling an exponential forgetting of the extent matrix [17]. That is,

$$\nu_{k+1|k} = 2d + 4 + e^{-T/\tau} (\nu_{k|k} - 2d - 4), \quad (5a)$$

$$V_{k+1|k} = \frac{\nu_{k+1|k} - 2d - 2}{\nu_{k|k} - 2d - 2} V_{k|k}, \quad (5b)$$

where T is the prediction time interval and τ the temporal decay constant. Note that (5a) is a modified version of the prediction update utilised in [10] to ensure the expected

value and covariance of the extent matrix are always well-defined [24].

Koch also proposed to solve the Chapman-Kolmogorov equation for a Wishart state transition density, and then to approximate the resulting Generalised Beta Type-II prediction density as an inverse Wishart distribution [10]. This idea was further built upon in [12], where an invertible parameter matrix is introduced to describe transformations of the extent matrix that are independent of the kinematic state vector. Moreover, a second-order moment matching technique is proposed to perform the inverse Wishart approximation [12], [25].

Granström *et al.* further generalised the idea of using a Wishart state transition density, presenting a prediction update that enables the evolution of the extent matrix to be functionally dependent upon the kinematic state vector [13]:

$$p(X_{k+1}|\mathbf{x}_k, X_k) = \mathcal{W}_d\left(X_{k+1}|n_{k+1}, \frac{M_{\mathbf{x}_k} X_k M_{\mathbf{x}_k}^T}{n_{k+1}}\right). \quad (6)$$

Here, the scalar design parameter $n_{k+1} > d-1$, and the matrix transformation $M_{\mathbf{x}_k} \triangleq M(\mathbf{x}_k)$ such that $M: \mathbb{R}^{n_x} \rightarrow \mathbb{R}^{d \times d}$ is a nonsingular matrix-valued function of the kinematic state vector [13]. In order to account for kinematic state uncertainty, the use of (6) leads to the following integral representation of the predicted extent matrix density:

$$p(X_{k+1}|\mathbf{Z}^k) = \int \mathcal{N}(\mathbf{x}_k|\mathbf{m}_{k|k}, P_{k|k}) \times \mathcal{G}_d^{II}\left(X_{k+1} \middle| \frac{n_{k+1}}{2}, \frac{\nu_{k|k} - 2d - 2}{2}, \frac{M_{\mathbf{x}_k} V_{k|k} M_{\mathbf{x}_k}^T}{n_{k+1}}, 0_d\right) d\mathbf{x}_k. \quad (7)$$

Unfortunately, the above integral has no analytical solution [13]. Hence, a series of Kullback-Leibler divergence minimisations is employed to approximate (7) as an inverse Wishart distribution [26]. To summarise:

$$p(X_{k+1}|\mathbf{Z}^k) \approx \mathcal{W}_d(X_{k+1}|\nu_{k+1|k}, V_{k+1|k}), \quad (8)$$

where, the scalar degrees of freedom $\nu_{k+1|k}$ and parameter matrix $V_{k+1|k}$ are functions of the expected values

$$C_1 = \int (M_{\mathbf{x}_k} V_{k|k} M_{\mathbf{x}_k}^T)^{-1} \mathcal{N}(\mathbf{x}_k|\mathbf{m}_{k|k}, P_{k|k}) d\mathbf{x}_k, \quad (9a)$$

$$C_2 = \int M_{\mathbf{x}_k} V_{k|k} M_{\mathbf{x}_k}^T \mathcal{N}(\mathbf{x}_k|\mathbf{m}_{k|k}, P_{k|k}) d\mathbf{x}_k. \quad (9b)$$

Note that the above definition of C_1 was first presented in [27], and results in a more efficient implementation of the prediction update of [13]². See [27, Table IV] for further details.

Granström *et al.* showed that the use of (6) offers significant improvement in the tracking of extended targets within unknown turn-rates when compared to [10]–[12], [25]. Nevertheless, even under the assumption that the time evolution is independent of the kinematic state vector, i.e., $M_{\mathbf{x}_k} = M_k$, the prediction update requires a Kullback-Leibler divergence minimisation or moment matching technique to approximate

²An intermediary Kullback-Leibler divergence minimisation was originally required to approximate the distribution of $M_{\mathbf{x}_k} V_{k|k} M_{\mathbf{x}_k}^T$ as a Wishart distribution [13, Section IV.C]. To do so, C_1 was defined as the expectation of the logarithmic determinant, and a numerical root finding procedure was performed to obtain the degrees of freedom s_{k+1} .

the Generalised Beta Type-II density as an inverse Wishart distribution [13], [27]. In order to remove the need for such density approximations, Bartlett *et al.* [14] proposed the following non-central inverse Wishart state transition density:

$$p(X_{k+1}|X_k, \mathbf{Z}^k) = \mathcal{IW}_d^{nc}(X_{k+1}|v_{k+1}, \Sigma_{k+1}, \Theta_{k+1}(X_k)), \quad (10)$$

where the degrees of freedom v_{k+1} , parameter matrix Σ_{k+1} , and non-centrality matrix $\Theta_{k+1}(X_k)$ are defined as follows:

$$v_{k+1} \in (2d, \nu_{k|k}) \cap \mathbb{N}, \quad (11a)$$

$$\Sigma_{k+1} = M_{k+1} Q_{k+1}^{-1} M_{k+1}^T, \quad (11b)$$

$$\Theta_{k+1}(X_k) = M_{k+1}^{-T} X_k^{-1} M_{k+1}^{-1}. \quad (11c)$$

Here, the nonsingular $d \times d$ transition matrix M_{k+1} is used to model transformations independent of the kinematic state vector, and $Q_{k+1} \in \mathbb{S}_{++}^d$ is used to model uncertainties in the extent matrix evolution; offering an additional $d(d+1)/2$ tunable parameters than previous works [14]. Moreover, the use of (10) guarantees the prediction density is of the desired inverse Wishart form (4c) with the following scalar degrees of freedom and parameter matrix:

$$\nu_{k+1|k} = v_{k+1}, \quad (12a)$$

$$V_{k+1|k} = M_{k+1} V_{k|k} (I_d + Q_k V_{k|k})^{-1} M_{k+1}^T. \quad (12b)$$

The main contribution of this paper is to propose a generalisation of (10) that allows for kinematic state dependent evolutions of the extent matrix; e.g., rotations and scaling. In doing so, the proposed prediction update does not suffer from the same levels of information loss as [13], [27], requires only a *single* Kullback-Leibler divergence minimisation, and offers an additional tuning parameter to model uncertainties in target shape more effectively.

III. PROBLEM FORMULATION

In Bayesian filtering, the prediction step consists of solving the following integral

$$p(\xi_{k+1}|\mathbf{Z}^k) = \int p(\xi_{k+1}|\xi_k, \mathbf{Z}^k) p(\xi_k|\mathbf{Z}^k) d\xi_k. \quad (13)$$

In order to obtain a closed-form solution to this integral, it is assumed in [14] that the evolution of the extent matrix is independent of the kinematic state vector. Albeit true for non-maneuvring behaviours, this assumption is often violated during constant or variable turn manoeuvres—in which the target extent rotates as a function of the turn-rate [13]. Therefore, in order to improve the tracking performance of manoeuvring targets, we will now account for such dependency.

Inspired by [13], the non-Markov state transition density $p(\xi_{k+1}|\xi_k, \mathbf{Z}^k)$ is expanded as follows³:

$$p(\xi_{k+1}|\xi_k, \mathbf{Z}^k) = p(\mathbf{x}_{k+1}|X_{k+1}, \mathbf{x}_k, \mathbf{Z}^k) \times p(X_{k+1}|\mathbf{x}_k, X_k, \mathbf{Z}^k), \quad (14a)$$

$$\approx p(\mathbf{x}_{k+1}|\mathbf{x}_k) p(X_{k+1}|\mathbf{x}_k, X_k, \mathbf{Z}^k). \quad (14b)$$

³Following [14], the state transition density is non-Markov, and thus retains the dependency upon the measurement set \mathbf{Z}^k . This action enables for greater flexibility in the selection of state transition parameters to model target shape uncertainties; see [14, Section IV.D] for further details.

The evolution of the kinematic state vector is assumed to be independent of the extent matrix. Hence, phenomena dictated by the target extent are deemed negligible; for example, wind resistance [17].

Given posterior (3a) and non-Markov state transition density (14b), equation (13) becomes

$$p(\xi_{k+1}|\mathbf{Z}^k) = \int p(\mathbf{x}_{k+1}|\mathbf{x}_k) \int p(X_{k+1}|\mathbf{x}_k, X_k) \times p(X_k|\mathbf{Z}^k)p(\mathbf{x}_k|\mathbf{Z}^k)dX_k d\mathbf{x}_k. \quad (15)$$

As previously stated, it is often desired in Bayesian filtering for the prediction density to belong to the same distribution class as the posterior—enabling for a finite set of statistics to be updated in Bayesian recursion rather than the entire distribution [28]. Therefore, given (3a), we require that the resulting prediction density of (15) possesses the same functional form as (4a). Unfortunately, this condition cannot be proven to hold in general. Thus, as in the pioneering works of Granström *et al.* [13], we approximate (15) to be the product of two independent equations: one for the kinematic state vector, and another for the extent matrix:

$$p(\mathbf{x}_{k+1}|\mathbf{Z}^k) = \int p(\mathbf{x}_{k+1}|\mathbf{x}_k)p(\mathbf{x}_k|\mathbf{Z}^k)d\mathbf{x}_k, \quad (16a)$$

$$p(X_{k+1}|\mathbf{Z}^k) = \iint p(X_{k+1}|\mathbf{x}_k, X_k, \mathbf{Z}^k)p(X_k|\mathbf{Z}^k) \times p(\mathbf{x}_k|\mathbf{Z}^k)dX_k d\mathbf{x}_k. \quad (16b)$$

We must now determine an appropriate state transition density for both the kinematic state vector and extent matrix such that the resulting prediction densities of (16a) and (16b) are multivariate Gaussian and inverse Wishart distributions respectively. Following [13], [29], the state transition density of the kinematic state vector is given by,

$$p(\mathbf{x}_{k+1}|\mathbf{x}_k) = \mathcal{N}(\mathbf{x}_{k+1}|f_{k+1}(\mathbf{x}_k), D_{k+1}), \quad (17)$$

where $f_{k+1}: \mathbb{R}^{n_x} \rightarrow \mathbb{R}^{n_x}$ is the nonlinear state transition function, and $D_{k+1} \in \mathbb{S}_{++}^{n_x}$ is the dynamic noise covariance matrix [30], [31]. Substituting the state transition density (17) and posterior (3b) into (16a), the extended Kalman filter is then used to approximate the resulting prediction density as a multivariate Gaussian distribution [32], [33]. That is,

$$p(\mathbf{x}_{k+1}|\mathbf{Z}^k) \approx \mathcal{N}(\mathbf{x}_{k+1}|\mathbf{m}_{k+1|k}, P_{k+1|k}), \quad (18a)$$

where the mean and covariance are given by

$$\mathbf{m}_{k+1|k} = f_{k+1}(\mathbf{m}_{k|k}), \quad (18b)$$

$$P_{k+1|k} = F_{k+1}P_{k|k}F_{k+1}^T + D_{k+1}, \quad (18c)$$

$$F_{k+1} = \nabla_{\mathbf{x}} f_{k+1}(\mathbf{x}) \Big|_{\mathbf{x}=\mathbf{m}_{k|k}}. \quad (18d)$$

The problem considered in this work is to derive an analogous closed-form prediction update for the extent matrix. More specifically, to determine a suitable non-Markov state transition density $p(X_{k+1}|\mathbf{x}_k, X_k, \mathbf{Z}^k)$ that can be used in (16b) to obtain the desired inverse Wishart distribution (4c) with minimal approximations. In addition, the chosen state transition density must offer a high degree of modelling flexibility, be physically interpretable, and encapsulate a wide subset of possible kinematic state dependencies.

IV. PREDICTION UPDATE

In this section, we introduce the state transition density and present the new prediction update of the extent matrix. We show that via a single Kullback-Leibler divergence minimisation, the resulting prediction density of (16b) is an inverse Wishart distribution; given the state transition density is a non-central inverse Wishart distribution. All supporting lemmata and corollaries are given in the Appendix.

A. The Extent Matrix State Transition Density

Motivated by [13], [14], we define the non-Markov state transition density of the extent matrix as the following non-central inverse Wishart distribution:

$$p(X_{k+1}|\mathbf{x}_k, X_k, \mathbf{Z}^k) = \mathcal{IW}_d^{nc}(X_{k+1}|v_{k+1}, \Sigma_{k+1}(\mathbf{x}_k), \Theta(\mathbf{x}_k, X_k)), \quad (19)$$

where the scalar degrees of freedom v_{k+1} , parameter matrix $\Sigma_{k+1}(\mathbf{x}_k)$, and non-centrality matrix $\Theta_{k+1}(\mathbf{x}_k, X_k)$ are defined as follows:

$$v_{k+1} \in (2d, \nu_{k|k}] \cap \mathbb{N}, \quad (20a)$$

$$\Sigma_{k+1}(\mathbf{x}_k) = M_{\mathbf{x}_k} Q_{k+1}^{-1} M_{\mathbf{x}_k}^T, \quad (20b)$$

$$\Theta_{k+1}(\mathbf{x}_k, X_k) = M_{\mathbf{x}_k}^{-T} X_k^{-1} M_{\mathbf{x}_k}^{-1}. \quad (20c)$$

The tuneable parameters of the non-Markov state transition density are thereby the degrees of freedom v_{k+1} , the symmetric positive definite noise matrix $Q_{k+1} \in \mathbb{S}_{++}^d$, and the matrix transformation $M_{\mathbf{x}_k} \triangleq M(\mathbf{x}_k)$; where $M: \mathbb{R}^{n_x} \rightarrow \mathbb{R}^{d \times d}$ is a nonsingular matrix-valued function of the kinematic state. To provide adequate meaning to these parameters in regard to extended target tracking, we shall now briefly discuss the underlying state transition model.

B. The Extent Matrix State Transition Model

The proposed state transition density is a generalisation of [14]. From Lemma 1, the state transition model governing (19) and describing the evolution of the extent matrix from time t_k to t_{k+1} is

$$X_{k+1}^{-\frac{1}{2}} = M_{\mathbf{x}_k}^{-T} \left(X_k^{-\frac{1}{2}} + n_{k+1}^{\frac{1}{2}} W_{k+1}^{\frac{1}{2}} \right), \quad (21a)$$

$$W_{k+1} \sim \mathcal{W}_d \left(W_{k+1}|n_{k+1}, \frac{Q_{k+1}}{n_{k+1}} \right), \quad (21b)$$

where $n_{k+1} = v_{k+1} - d - 1$. Although model (21) seems rather complex, its physical interpretation can be separated into two simple components: the injection of Wishart distributed process noise W_{k+1} , and the extent evolution described by the transition matrix $M_{\mathbf{x}_k}$ [14]. We shall now discuss each of these components to highlight the properties of each state transition parameter.

In accordance with [23, Theorem 3.3.15], the expectation and variance of the process noise W_{k+1} is given by:

$$\mathbb{E}[W_{k+1}] = Q_{k+1}, \quad (22a)$$

$$\text{Var}(W_{k+1}) = \frac{Q_{k+1}Q_{k+1}}{v_{k+1}-d-1} + \frac{\text{tr}(Q_{k+1})Q_{k+1}}{v_{k+1}-d-1}. \quad (22b)$$

By (22), the primary parameter that governs the size, shape, and expected value of the process noise is the noise matrix Q_{k+1} [14]. Therefore, contrary to [13], [27], our model offers an additional $d(d+1)/2$ tunable parameters to describe the effects of process noise on the extent matrix evolution. For example, varying levels of process noise can be applied to each principle axis of the target extent; which can aid in the tracking of group targets such as truck convoys [14].

Furthermore, as Q_{k+1} approaches $0_{d,d}$, the expected value and variance of the process noise also approach $0_{d,d}$ (22). This implies that, although non-linearly, smaller elements of Q_{k+1} results in a more deterministic evolution of the target extent [14]. Hence, the noise matrix Q_{k+1} is analogous to the dynamic noise covariance matrix D_{k+1} (17); which models the uncertainty in the evolution of the kinematic state vector \mathbf{x}_k from time t_k to t_{k+1} . In Section IV-D, we shall provide methodologies for tuning v_{k+1} and Q_{k+1} for extended target tracking purposes.

Once the process noise W_{k+1} has been injected, the state transition model then performs the evolution described by $M_{\mathbf{x}_k}$. To highlight the effects of $M_{\mathbf{x}_k}$, consider the ideal scenario in which the process noise is zero. Then, (21a) is equivalent to the deterministic model

$$X_{k+1} = M_{\mathbf{x}_k} X_k M_{\mathbf{x}_k}^T. \quad (23)$$

Thus, as in the works of [13], the main motivation for $M_{\mathbf{x}_k}$ is to model rotations of the target extent; however, in general, the function $M_{\mathbf{x}_k}$ can be selected as any arbitrary transformation—provided the output is a non-singular $d \times d$ matrix [14]. For example, in group target tracking the group extent may grow or shrink over time, corresponding to $M_{\mathbf{x}_k}$ to be a scale matrix [17]. The matrix transformation $M_{\mathbf{x}_k}$ is thereby analogous to the kinematic state transition function f_{k+1} (17); which models the evolution of the kinematic state vector \mathbf{x}_k from time t_k to t_{k+1} . Within our work, we shall consider $M_{\mathbf{x}_k}$ to be of the following form:

$$M_{\mathbf{x}_k} = \begin{bmatrix} \cos(T\omega_k) & -\sin(T\omega_k) \\ \sin(T\omega_k) & \cos(T\omega_k) \end{bmatrix}, \quad (24)$$

where T is the time interval, $\mathbf{x}_k = [x_k, y_k, \dot{x}_k, \dot{y}_k, \omega_k]^T$, and ω_k is the turn-rate of the extended target. Note that (24) is commonly utilised to model target extent rotations; see e.g., [13], [16], [27], [29].

C. The Generalised Extent Matrix Prediction Update

Substituting the posterior (3) and the state transition density (19) into (16b), the prediction update of the extent matrix is equivalent to

$$p(X_{k+1}|\mathbf{Z}^k) = \iint \mathcal{IW}_d^{nc}(X_{k+1}|v_{k+1}, \Sigma_{k+1}(\mathbf{x}_k), \Sigma_{k+1}(\mathbf{x}_k)\Theta(\mathbf{x}_k, X_k)) \times \mathcal{N}(\mathbf{x}_k|\mathbf{m}_{k|k}, P_{k|k}) \mathcal{IW}_d(X_k|v_{k|k}, V_{k|k}) dX_k d\mathbf{x}_k, \quad (25)$$

which, given [14, Theorem 1], yields the intermediate integral

$$p(X_{k+1}|\mathbf{Z}^k) = \int \mathcal{N}(\mathbf{x}_k|\mathbf{m}_{k|k}, P_{k|k}) \times \mathcal{IW}_d(X_k|v_{k+1}, M_{\mathbf{x}_k} \bar{V}_{k+1} M_{\mathbf{x}_k}^T) d\mathbf{x}_k, \quad (26a)$$

where the intermediate parameter matrix $\bar{V}_{k+1} \in \mathbb{S}_{++}^d$ is

$$\bar{V}_{k+1} = V_{k|k}(I_d + Q_{k+1}V_{k|k})^{-1}. \quad (26b)$$

Unfortunately, the above integral (26a) has no analytical solution. Hence, motivated by [13], we resort to approximating the resulting prediction density with an inverse Wishart distribution through Kullback-Leibler divergence minimisation.

Kullback-Leibler divergence is considered the optimal difference measure when approximating distributions in a maximum likelihood sense [34]–[36]. For the two distributions $p(X)$ and $q(X)$, the Kullback-Leibler divergence is defined as follows [37]:

$$\text{KL}(p(X)||q(X)) = \int p(X) \log\left(\frac{p(X)}{q(X)}\right) dX. \quad (27)$$

By defining $p(X)$ as (26a) and $q(X)$ by (4c), Lemma 2 proves that the best and unique global approximation of (26a) that minimises (27) is given by

$$p(X_{k+1}|\mathbf{Z}^k) \approx \mathcal{IW}_d(X_{k+1}|v_{k+1|k}, V_{k+1|k}), \quad (28a)$$

where the parameter matrix $V_{k+1|k}$ is equal to

$$V_{k+1|k} = \left(\frac{v_{k+1|k} - d - 1}{v_{k+1} - d - 1}\right) C_1^{-1}, \quad (28b)$$

and the scalar degrees of freedom $v_{k+1|k}$ is the solution to

$$d \ln\left(\frac{v_{k+1|k} - d - 1}{v_{k+1} - d - 1}\right) + \sum_{i=1}^d \psi_0\left(\frac{v_{k+1} - d - i}{2}\right) - \sum_{i=1}^d \psi_0\left(\frac{v_{k+1|k} - d - i}{2}\right) - C_3 - \ln(|C_1|) = 0. \quad (28c)$$

Furthermore, C_1 and C_3 are the expectations

$$C_1 = \int (M_{\mathbf{x}_k} \bar{V}_{k+1} M_{\mathbf{x}_k}^T)^{-1} \mathcal{N}(\mathbf{x}_k|\mathbf{m}_{k|k}, P_{k|k}) d\mathbf{x}_k, \quad (28d)$$

$$C_3 = \int \ln(|M_{\mathbf{x}_k} \bar{V}_{k+1} M_{\mathbf{x}_k}^T|) \mathcal{N}(\mathbf{x}_k|\mathbf{m}_{k|k}, P_{k|k}) d\mathbf{x}_k. \quad (28e)$$

The optimal value of the scalar degrees of freedom $v_{k+1|k}$ can be found by applying a numerical root-finding algorithm to (28c). Examples include the Newton-Raphson algorithm and Halley's method [38]. Nevertheless, to improve the computational efficiency of the prediction update, we shall utilise the following theorem to obtain a closed-form solution for $v_{k+1|k}$.

Theorem 1. The expected values of (26a) and (28a) will have the same volume if the scalar degrees of freedom $v_{k+1|k}$ is

$$v_{k+1|k} = 2d + 2 + \frac{(d+1)\rho_{k+1}}{(\rho_{k+1} + d + 1)|C_1 C_2|^{\frac{1}{d}} - \rho_{k+1}}, \quad (29)$$

where $\rho_{k+1} = v_{k+1} - 2d - 2$, and the expectation

$$C_2 = \int M_{\mathbf{x}_k} \bar{V}_{k+1} M_{\mathbf{x}_k}^T \mathcal{N}(\mathbf{x}_k|\mathbf{m}_{k|k}, P_{k|k}) d\mathbf{x}_k. \quad (30)$$

Proof. Let $\bar{\mathbb{E}}[X_{k+1}|\mathbf{Z}^k]$ and $\mathbb{E}[X_{k+1}|\mathbf{Z}^k]$ denote the expected values of (26a) and (28a) respectively. By [23, Theorem 3.4.3],

$$\bar{\mathbb{E}}[X_{k+1}|\mathbf{Z}^k] = \frac{C_2}{\nu_{k+1} - 2d - 2}, \quad (31a)$$

$$\mathbb{E}[X_{k+1}|\mathbf{Z}^k] = \frac{V_{k+1|k}}{\nu_{k+1|k} - 2d - 2}. \quad (31b)$$

The volume of an ellipsoid X is equal to $c_d|X|$ where c_d is the volume of a d -dimensional unit sphere [14]. Matching the volume of the expected values is thereby equivalent to matching the determinants

$$\left| \frac{V_{k+1|k}}{\nu_{k+1|k} - 2d - 2} \right| = \left| \frac{C_2}{\nu_{k+1} - 2d - 2} \right|. \quad (32)$$

Substituting (28b) into (32) and re-arranging yields (29). \square

As stated previously, the main motivation for $M_{\mathbf{x}_k}$ is to model rotations of the target extent. Thus, to compare the optimal (28c) and closed-form (29) solutions of $\nu_{k+1|k}$, we define $M_{\mathbf{x}_k}$ by (24). Furthermore, motivated by [13, Corollary 2], we approximate the expectations C_1 , C_2 , and C_3 with third-order Taylor series expansions. That is, given $\mathbb{V}_{\mathbf{x}_k} \triangleq M_{\mathbf{x}_k} \bar{V}_{k+1} M_{\mathbf{x}_k}^T$:

$$C_1 \approx \left(\mathbb{V}_{\mathbf{x}_k}^{-1} + \sum_{i=1}^{n_x} \sum_{j=1}^{n_x} \frac{\partial^2 \mathbb{V}_{\mathbf{x}_k}^{-1}}{\partial \mathbf{x}_k^i \partial \mathbf{x}_k^j} P_{k|k}^{ij} \right) \Big|_{\mathbf{x}_k = \mathbf{m}_{k|k}}, \quad (33a)$$

$$C_2 \approx \left(\mathbb{V}_{\mathbf{x}_k} + \sum_{i=1}^{n_x} \sum_{j=1}^{n_x} \frac{\partial^2 \mathbb{V}_{\mathbf{x}_k}}{\partial \mathbf{x}_k^i \partial \mathbf{x}_k^j} P_{k|k}^{ij} \right) \Big|_{\mathbf{x}_k = \mathbf{m}_{k|k}}, \quad (33b)$$

$$C_3 \approx \left(\ln(|\mathbb{V}_{\mathbf{x}_k}|) + \sum_{i=1}^{n_x} \sum_{j=1}^{n_x} \frac{\partial^2 \ln(|\mathbb{V}_{\mathbf{x}_k}|)}{\partial \mathbf{x}_k^i \partial \mathbf{x}_k^j} P_{k|k}^{ij} \right) \Big|_{\mathbf{x}_k = \mathbf{m}_{k|k}}, \quad (33c)$$

where \mathbf{x}_k^i denotes the i^{th} element of \mathbf{x}_k , and $P_{k|k}^{ij}$ denotes the $(i, j)^{\text{th}}$ element of $P_{k|k}$.

Figure 1 shows the optimal and closed-form solutions of $\nu_{k+1|k}$ for differing levels of turn-rate variance $P_{k|k}^{\omega}$ and state transition degrees of freedom ν_{k+1} . The intermediate parameter matrix $\bar{V}_{k+1} = \text{diag}([10^2, 5^2])$, and the expected value of the turn-rate $\omega_{k|k} = 10^\circ/T$. From Figure 1b, it is observed that the maximum relative error between the optimal and closed-form solutions is less than ten percent. We remark here that relative error experienced between the optimal and closed-form solutions proposed in [13] is *typically on the order of one tenth of a degree of freedom*; see [13, Corollary 1]. We thereby conclude that, as in the works of [13], our closed-form solution is an adequate approximation to the optimal solution.

In addition to the above discussion, the closed-form solution (29) ensures the volume of the expected value of the extent matrix remains constant over the inverse Wishart approximation. Furthermore, by Jensen's inequality, the expected value of the extent matrix is always well-defined. That is, the closed-form solution guarantees $\nu_{k+1|k} > 2d + 2$. We remark

⁴By (24), the matrix transformation $M_{\mathbf{x}_k}$ is a function of the turn-rate ω_k and prediction time interval T . Therefore, no covariance element other than turn-rate variance will impact the expectations C_1 , C_2 , and C_3 .

TABLE II: Proposed Prediction Update

Input: Previous kinematic state estimate, covariance, degrees of freedom, and parameter matrix $\{\mathbf{m}_{k|k}, P_{k|k}, \nu_{k|k}, V_{k|k}\}$. Kinematic state transition function and covariance $\{f_{k+1}, D_{k+1}\}$. Extent matrix state transition parameters and transformation $\{\nu_{k+1}, Q_{k+1}, M_{\mathbf{x}_k}\}$.
Output: $\{\mathbf{m}_{k+1|k}, P_{k+1|k}, \nu_{k+1|k}, V_{k+1|k}\}$.

$$\begin{aligned} \mathbf{m}_{k+1|k} &= f_{k+1}(\mathbf{m}_{k|k}), \\ P_{k+1|k} &= F_{k+1} P_{k|k} F_{k+1}^T + D_{k+1}, \\ \nu_{k+1|k} &= 2d + 2 + \frac{(d+1)\rho_{k+1}}{(\rho_{k+1} + d + 1)|C_1 C_2|^{\frac{1}{d}} - \rho_{k+1}}, \end{aligned}$$

$$V_{k+1|k} = \left(\frac{\nu_{k+1|k} - d - 1}{\nu_{k+1} - d - 1} \right) C_1^{-1},$$

$$\bar{V}_{k+1} = V_{k|k} (I_d + Q_{k+1} V_{k|k})^{-1},$$

$$\rho_{k+1} = \nu_{k+1} - 2d - 2,$$

$$F_{k+1} = \nabla_{\mathbf{x}} f_{k+1}(\mathbf{x}) \Big|_{\mathbf{x} = \mathbf{m}_{k|k}},$$

$$C_1 = \int (M_{\mathbf{x}_k} \bar{V}_{k+1} M_{\mathbf{x}_k}^T)^{-1} \mathcal{N}(\mathbf{x}_k | \mathbf{m}_{k|k}, P_{k|k}) d\mathbf{x}_k,$$

$$C_2 = \int M_{\mathbf{x}_k} \bar{V}_{k+1} M_{\mathbf{x}_k}^T \mathcal{N}(\mathbf{x}_k | \mathbf{m}_{k|k}, P_{k|k}) d\mathbf{x}_k.$$

here that the same cannot be said for the optimal solution; which only guarantees $\nu_{k+1|k} > 2d$. The proposed prediction update is presented in Table II. To avoid numerical root-finding and ensure the expected value is well-defined, the update uses Theorem 1.

D. Parameter Selection

In this section, we discuss methodologies to select the state transition parameters to model practical phenomena. Before presenting said methodologies however, we first remark that the extent matrix state transition density (19) is non-Markov. This enables for the state transition parameters ν_{k+1} and Q_{k+1} to be functionally dependent upon the posterior parameters $V_{k|k}$ and $\nu_{k|k}$.

The first setting introduced for the state transition degrees of freedom is

$$\nu_{k+1} = 2d + 2 + (\nu_{k|k} - 2d - 2) |I_d + Q_{k+1} V_{k|k}|^{-\frac{1}{d}}. \quad (35)$$

In accordance with [14], the above setting ensures that the volume of the expected value of the extent matrix is preserved for all Q_{k+1} . Nevertheless, the volume is still dependent upon the matrix transformation $M_{\mathbf{x}_k}$. Specifically, by Lemma 9,

$$\begin{aligned} \text{Vol}(\mathbb{E}[X_{k+1}|\mathbf{Z}^k]) &= \\ \text{Vol} \left(\int M_{\mathbf{x}_k} \mathbb{E}[X_k|\mathbf{Z}^k] H M_{\mathbf{x}_k}^T \mathcal{N}(\mathbf{x}_k | \mathbf{m}_{k|k}, P_{k|k}) d\mathbf{x}_k \right), \end{aligned} \quad (36)$$

where $H \triangleq (I_d + Q_{k+1} V_{k|k})^{-1} |I_d + Q_{k+1} V_{k|k}|^{\frac{1}{d}} \in \mathbb{S}\mathbb{L}(d, \mathbb{R})$.

From (36), it can be seen that the variance of the kinematic state vector influences the volume of the expected value. As the variance increases, so to will the expected volume. The setting is thereby suitable for modelling changes in target size that are dependent upon the kinematic state vector. For example, the spread of a truck convoy may be dependent upon the convoy

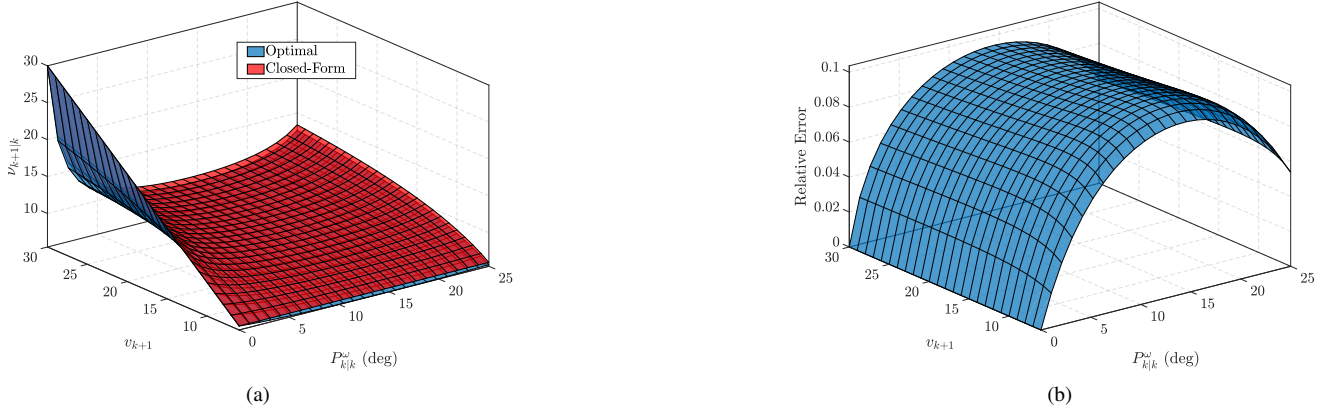


Fig. 1: (a) The optimal (blue) and closed-form (red) solutions of $\nu_{k+1|k}$ for differing levels of turn-rate variance $P_{k|k}^\omega$ and state transition degrees of freedom v_{k+1} . (b) The relative error between the optimal and closed-form solutions.

speed or acceleration⁵. Assuming $M_{\mathbf{x}_k}$ is an appropriate scale matrix, equation (35) ensures that the size of the truck convoy is adequately updated based upon the current estimate of the kinematic state. Similarly, the shape of the truck convoy can be adequately modified through the noise matrix Q_{k+1} to handle any unforeseen transformations of the group extent. We refer the reader to [14, Section IV-D] for further details on the selection of noise matrix Q_{k+1} to model practical phenomena.

In contrast to the above discussion, the volume of an extended target may be time invariant. For example, the volume of a surface vessel or ground vehicle will not change over time. Hence, it would be desirable to ensure the volume of the expected value of the extent matrix is preserved from time t_k to t_{k+1} . This gives motivation for the following setting of the state transition degrees of freedom;

$$v_{k+1} = 2d + 2 + (\nu_{k|k} - 2d - 2) |C_2^{-1} V_{k|k}|^{-\frac{1}{d}}. \quad (37)$$

The above setting ensures that the volume of the expected value of the extent matrix is preserved for all Q_{k+1} and $M_{\mathbf{x}_k}$. That is,

$$\text{Vol}(\mathbb{E}[X_{k+1} | \mathbf{Z}^k]) = \text{Vol}(\mathbb{E}[X_k | \mathbf{Z}^k]). \quad (38)$$

Given setting (37), it is assumed that the kinematic state vector only influences the shape and orientation of the target extent. All influences in size are neglected. We remark here that any unforeseen evolutions in target shape can still be adequately modelled by the noise matrix Q_{k+1} . Furthermore, if $M_{\mathbf{x}_k}$ is independent of \mathbf{x}_k and $|M_{\mathbf{x}_k}| = 1$, (37) reduces to (35).

V. SIMULATIONS

This section presents several simulated results that compare the proposed prediction update to [13], [14]. The works of [12] have been excluded from this section, as the prediction update of [14] was shown to outperform [12] whenever the turn-rate is unknown to the observer; see [14, Section VII] for further discussion.

⁵In general, the distance between each truck will increase as a function of the convoy speed or acceleration. Hence, the overall size of the truck convoy must be modified accordingly.

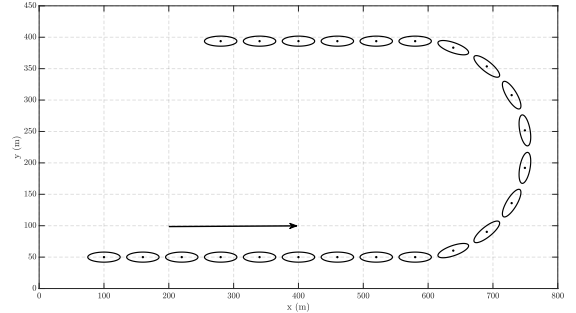


Fig. 2: Trajectory of an extended target. Shown are, for every second scan k , the true target position and the true target extent.

A. Constant Turn Manoeuvre

A single extended target followed the trajectory shown in Figure 2. The target extent was represented by an ellipsoid with diameters 50m and 16m respectively. The speed of the extended target was assumed constant at 30m/s. At time-step $k = 18$, the extended target performed a constant turn manoeuvre with a turn-rate of $10^\circ/\text{s}$. Scattering measurement centers were uniformly distributed over the target extent X_k , and the measurement noise was assumed to be zero-mean Gaussian distributed with covariance $R_k = \text{diag}([1.5^2, 1.5^2])$. The number of measurements at each time step was Poisson distributed with mean 10, and the scan rate was $T = 1\text{s}$.

Herein, the prediction of [14] is denoted by M1. A white noise acceleration model was used to update the kinematic state vector; which contained the Cartesian position and velocity of the extended target. That is, $\mathbf{x}_k = [x_k, y_k, \dot{x}_k, \dot{y}_k]^T$. We remark here that M1 assumes a conditional random matrix model, therefore, unlike its competitors, the turn-rate of the extended target cannot be included within the kinematic state vector. The three discrete models of M1 were chosen to adopt

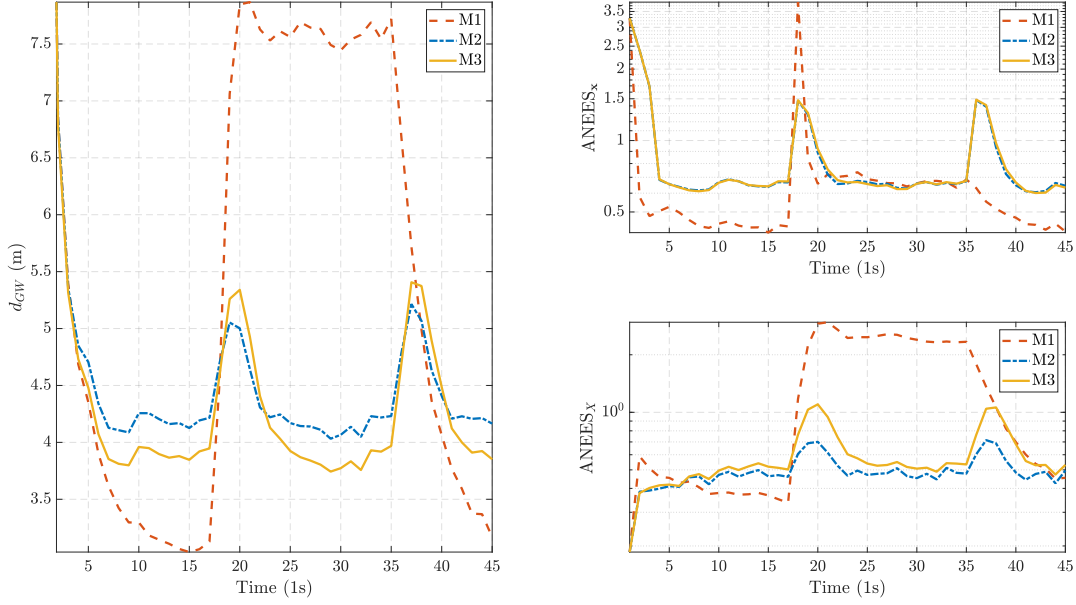


Fig. 3: The Gaussian Wasserstein distance (left) and ANEES (right) over 900 Monte Carlo runs. The red dashed line is approach M1, the blue dash-dot line is approach M2 and the yellow solid line is approach M3.

the following parameters⁶:

- 1) π_1 : Low kinematic and extent process noise; $\tilde{q} = 0.001\text{m}^2/\text{s}^3$ and $Q_{k+1} = 0.2V_{k|k}^{-1}$,
- 2) π_2 : Medium kinematic and extent process noise; $\tilde{q} = 3\text{m}^2/\text{s}^3$ and $Q_{k+1} = 0.33V_{k|k}^{-1}$,
- 3) π_3 : High kinematic and extent process noise; $\tilde{q} = 6.75\text{m}^2/\text{s}^3$ and $Q_{k+1} = 1.25|V_{k|k}|^{-\frac{1}{d}}I_d$.

It was assumed no prior information was known in regard to the turn-rate manoeuvre. Thus, the transition matrix M_{k+1} was chosen to be (24) with $\sigma_{k+1} = 1$ and $\theta = 0^\circ$ for each model.

Henceforth, the estimators using the prediction update of [13] and the proposed prediction update are denoted by M2 and M3 respectively. To remove any potential bias, the correction step of Feldmann *et al.* [11] was used by both estimators. Furthermore, a constant turn model was used to update the kinematic state vector of M2 and M3; which contained the Cartesian position, velocity, and turn-rate of the extended target. That is, $\mathbf{x}_k = [x_k, y_k, \dot{x}_k, \dot{y}_k, \omega_k]^T$. The parameters of the two estimators were chosen as follows:

- 1) M2: Medium kinematic and extent process noise; $\sigma_a = 2.0$, $\sigma_\omega = 0.1^\circ$, and $n_{k+1} = 30$,
- 2) M3: Medium kinematic and extent process noise; $\sigma_a = 2.0$, $\sigma_\omega = 0.1^\circ$, and $Q_{k+1} = 0.33V_{k|k}^{-1}$,

where σ_a and σ_ω denote the standard deviation of the target acceleration and turn-rate respectively; see [31] for details. Furthermore, for M3, the state transition degrees of freedom v_{k+1} was set according to (37).

⁶Here, \tilde{q} denotes the process noise intensity, and is required when using the discrete-time equivalent white noise acceleration model; see [31] for details. In accordance with Feldmann *et al.* [11], we define $\tilde{q} \triangleq 0.75T\sigma_a^2$, where σ_a denotes the standard deviation of the target acceleration.

To evaluate the tracking performance of each estimator, we exploit two credibility measures over $N = 900$ Monte Carlo runs. The first credibility measure is the Gaussian Wasserstein distance d_{GW} , which is the recommended metric for comparing elliptical extended targets [17], [39]. The square of the Gaussian Wasserstein distance is given by:

$$d_{GW}^2 = \frac{1}{N} \sum_{i=1}^N \left(\text{tr}(X_k + \bar{X}_{k|k} - 2\hat{X}_k) + \|\mathbf{m}_{k|k} - \mathbf{x}_k\|^2 \right), \quad (39)$$

where $\bar{X}_{k|k} = V_{k|k}/(v_{k|k} - 2d - 2)$, and $\hat{X}_k = (X_k^{\frac{1}{2}} \bar{X}_{k|k} X_k^{\frac{1}{2}})^{\frac{1}{2}}$.

The second credibility measure is the average normalised estimation error squared (ANEES), which measures how confident an estimator is in its estimation quality [11]. Values greater than one indicate that the estimator is overly confident, whilst values less than one indicate that the estimator is too pessimistic. The ANEES of the kinematic state vector and the extent matrix are calculated as follows:

$$\text{ANEES}_x = \frac{1}{Nn_x} \sum_{i=1}^N (\mathbf{m}_{k|k} - \mathbf{x}_k)^T P_{k|k} (\mathbf{m}_{k|k} - \mathbf{x}_k), \quad (40a)$$

$$\text{ANEES}_X = \frac{1}{N} \sum_{i=1}^N \frac{\text{Tr}((X_{k|k} - X_k)^2)}{e_{k|k}}, \quad (40b)$$

where $e_{k|k} \triangleq \text{Tr}(\text{Var}(X_k | \mathcal{Z}^k))$ [11].

Figure 3 shows the results of each estimator. Due to the use of a white noise acceleration model, M1 offers the best target tracking performance during the constant velocity motion. Nevertheless, during the turn-rate manoeuvre, both M2 and M3 offer significant improvement in target tracking performance than M1. This performance increase can be attributed to two key points. Firstly, the use of a constant-turn model to

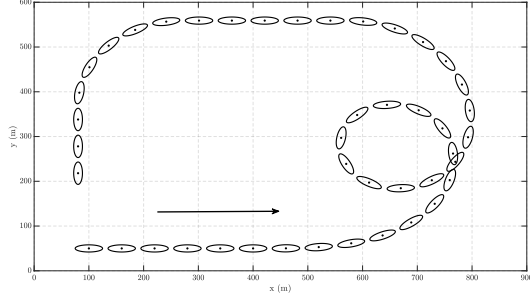


Fig. 4: Trajectory of an extended target. Shown are, for every second scan k , the true target position and the true target extent.

update the kinematic state vector, and secondly, the use of the matrix transformation $M_{\mathbf{x}_k}$ (24) to update the orientation of target extent. Moreover, the ANEES of the target extent is significantly larger for M1 than the other two estimators. This indicates that M1 experiences greater levels of overconfidence in its estimation quality than M2 and M3; particularly for the target extent.

B. Variable Turn Manoeuvre

In this simulation, the extended target followed the trajectory presented in Figure 4. As this trajectory involves long sequences of variable and constant turn-maneuvres, we have restricted our simulation to compare only the factorised estimators M2 and M3. The parameters of each estimator were set to the same values as in the previous simulation.

Figure 5 shows the results of each estimator. Interestingly, M3 possesses a lower Gaussian Wasserstein distance than M2 for a significant portion of the simulation, with a maximum relative difference of $\approx 8.7\%$ (left). This could be a benefit of using a single Kullback-Leibler divergence minimisation as opposed to several, or due to preserving the volume of the expected extent matrix via the state transition degrees of freedom v_{k+1} . In regard to the ANEES, both estimators appear to be too over-confident in their estimation quality of the kinematic state vector (top right); particularly in the last sequence of constant velocity and constant turn motions. For the target extent, the ANEES of both estimators never exceeds a value of one. We also note that the ANEES of M3 is much larger than M2; with a maximum relative difference of $\approx 32.7\%$ (bottom right). This indicates that M3 is less pessimistic than M2, and therefore possesses a better level of confidence in its estimation quality of the target extent.

VI. CONCLUDING REMARKS

In this contribution, we generalised the prediction update presented [14] to enable for kinematic state dependent evolutions of the target extent. In contrast to [13], the newly proposed update required the use of only a *single* Kullback-Leibler divergence minimisation, and offers an additional tuning parameter to model target shape uncertainties—the noise matrix Q_{k+1} . To avoid numerical root-finding, we additionally

provided a closed-form solution for the predicted degrees of freedom $\nu_{k+1|k}$. Further, we presented two alternatives on the selection of the state transition degrees of freedom v_{k+1} to model practical phenomena. Simulated results indicate that the proposed prediction update enables for improved target tracking performance than previous works.

Although not utilised to its full potential, the noise matrix can be utilised to model transformations of the target extent. Future research should be pushed in this direction to determine other potential structures of Q_{k+1} which can aid in the tracking of extended and group targets.

APPENDIX

Lemma 1. Let the non-Markov state transition density $p(X_{k+1}|\mathbf{x}_k, X_k, \mathbf{Z}^k)$ be the non-central inverse Wishart distribution described in (19). Then, the state transition model governing the evolution of X_k to X_{k+1} is

$$X_{k+1}^{-\frac{1}{2}} = M_{\mathbf{x}_k}^{-T} \left(X_k^{-\frac{1}{2}} + n_{k+1}^{\frac{1}{2}} W_{k+1}^{\frac{1}{2}} \right), \quad (41a)$$

$$W_{k+1} \sim \mathcal{W}_d \left(W_{k+1} | n_{k+1}, \frac{Q_{k+1}}{n_{k+1}} \right), \quad (41b)$$

where $n_{k+1} \triangleq v_{k+1} - d - 1$.

Proof. Let $X_k^{-1} = Y_k Y_k^T$, where Y_k is a real $d \times n_k$ matrix with dimension $n_k \triangleq \nu_{k|k} - d - 1$. By [14, Lemma 2],

$$X_k^{-1} = Y_k Y_k^T = (Y_k H_1^T) (Y_k H_1^T)^T, \quad (42)$$

where $H_1 \in \mathbb{O}^{n_{k+1} \times n_k}$ with $n_{k+1} \triangleq v_{k+1} - d - 1$. Similarly, let $X_{k+1}^{-1} = Y_{k+1} Y_{k+1}^T$, where Y_{k+1} is a real $d \times n_{k+1}$ matrix. Then, using [14, Lemma 3], (19) is equivalent to

$$p(Y_{k+1}|\mathbf{x}_k, Y_k, \mathbf{Z}^k) = \mathcal{N}_{d, n_{k+1}} \left(Y_{k+1} | M_{\mathbf{x}_k}^{-T} Y_k H_1^T, \Sigma_{\mathbf{x}_k}^{-1} \otimes I_{n_{k+1}} \right), \quad (43)$$

where $\Sigma_{\mathbf{x}_k} = M_{\mathbf{x}_k} Q_{k+1}^{-1} M_{\mathbf{x}_k}^T$ (20b). The state transition model governing (43) is given by:

$$Y_{k+1} = M_{\mathbf{x}_k}^{-T} \left(Y_k H_1^T + n_{k+1}^{\frac{1}{2}} U_{k+1} \right), \quad (44a)$$

$$U_{k+1} \sim \mathcal{N}_{d, n_{k+1}} \left(U_{k+1} | 0_{d, n_{k+1}}, \frac{Q_{k+1}}{n_{k+1}} \otimes I_{n_{k+1}} \right). \quad (44b)$$

Define $X_k^{-\frac{1}{2}} = Y_k H_1^T$, $X_{k+1}^{-\frac{1}{2}} = Y_{k+1}$, and $W_{k+1}^{\frac{1}{2}} = U_{k+1}$. Then, according to [23, Theorem 3.2.2], the state transition model governing the evolution of X_k to X_{k+1} is given by:

$$X_{k+1}^{-\frac{1}{2}} = M_{\mathbf{x}_k}^{-T} \left(X_k^{-\frac{1}{2}} + n_{k+1}^{\frac{1}{2}} W_{k+1}^{\frac{1}{2}} \right), \quad (45a)$$

$$W_{k+1} \sim \mathcal{W}_d \left(W_{k+1} | n_{k+1}, \frac{Q_{k+1}}{n_{k+1}} \right); \quad (45b)$$

which is the desired result. \square

Lemma 2. Consider the probability density function

$$p(X) = \int \mathcal{I} \mathcal{W}_d(X | v, M_{\mathbf{x}} \bar{V} M_{\mathbf{x}}^T) \mathcal{N}(\mathbf{x} | \mathbf{m}, P) d\mathbf{x}, \quad (46)$$

where $M_{\mathbf{x}} \triangleq M(\mathbf{x})$ such that $M: \mathbb{R}^{n_x} \rightarrow \mathbb{R}^{d \times d}$ is a non-singular matrix-valued function. Moreover, let (ν^*, V^*) denote the parameter set that minimises the Kullback-Leibler

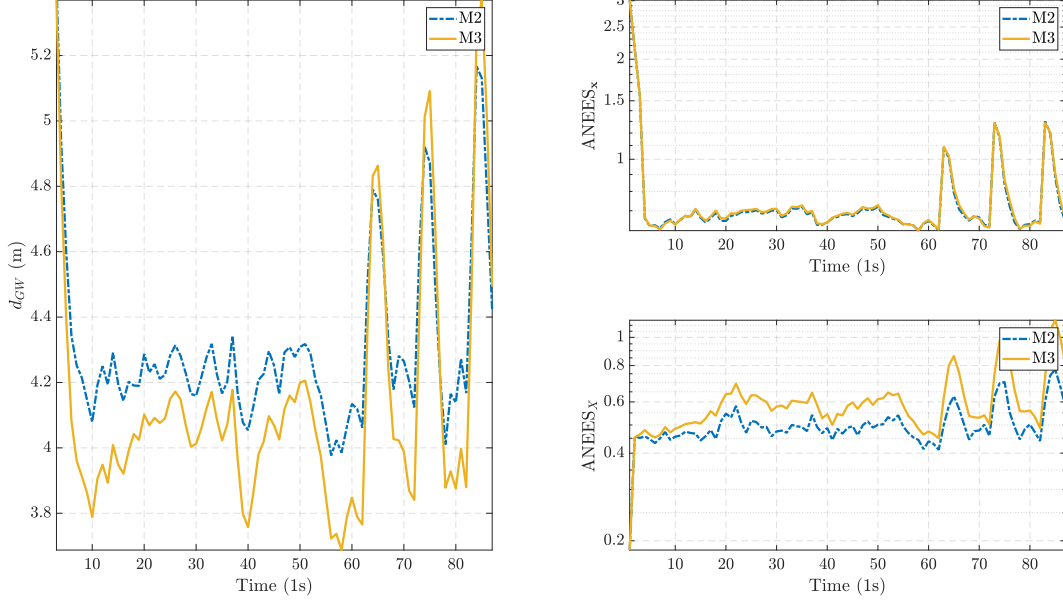


Fig. 5: The Gaussian Wasserstein distance (left) and ANEES (right) over 900 Monte Carlo runs. The blue dash-dot line is approach M2 and the yellow solid line is approach M3.

divergence between $p(X)$ and all inverse Wishart distributions \mathcal{IW}_d ; i.e.,

$$(\nu^*, V^*) = \arg \min_{(\nu, V)} \text{KL}(p(X) || \mathcal{IW}_d(X | \nu, V)). \quad (47)$$

Then, the matrix V^* is given by

$$V^* = \left(\frac{\nu^* - d - 1}{\nu^* - d - 1} \right) C_1^{-1}, \quad (48)$$

and ν^* is the solution to

$$d \ln \left(\frac{\nu^* - d - 1}{\nu^* - d - 1} \right) + \sum_{i=1}^d \psi_0 \left(\frac{\nu^* - d - i}{2} \right) - \sum_{i=1}^d \psi_0 \left(\frac{\nu^* - d - i}{2} \right) - C_3 - \ln(|C_1|) = 0, \quad (49)$$

where C_1 and C_3 are the expectations:

$$C_1 = \int (M_{\mathbf{x}} \bar{V} M_{\mathbf{x}}^T)^{-1} \mathcal{N}(\mathbf{x} | \mathbf{m}, P) d\mathbf{x}, \quad (50a)$$

$$C_3 = \int \ln(|M_{\mathbf{x}} \bar{V} M_{\mathbf{x}}^T|) \mathcal{N}(\mathbf{x} | \mathbf{m}, P) d\mathbf{x}. \quad (50b)$$

Proof. By equation (27),

$$(\nu^*, V^*) = \arg \min_{(\nu, V)} \text{KL}(p(X) || \mathcal{IW}_d(X | \nu, V)), \quad (51a)$$

$$\equiv \arg \max_{(\nu, V)} \int p(X) \ln(\mathcal{IW}_d(X | \nu, V)) dX, \quad (51b)$$

$$\equiv \arg \max_{(\nu, V)} f(\nu, V), \quad (51c)$$

where the objective function

$$f(\nu, V) = \frac{\nu - d - 1}{2} (\ln(|V|) - d \ln(2)) - \frac{\nu}{2} \mathbb{E}[\ln(|X|)] - \frac{1}{2} \text{tr}(V \mathbb{E}[X^{-1}]) - \ln \left(\Gamma_d \left(\frac{\nu - d - 1}{2} \right) \right). \quad (52)$$

The first-order necessary condition for optimality requires that the gradient of the object function (52) will be zero. Therefore, (ν^*, V^*) must satisfy

$$\nabla f(\nu, V) = \left[\frac{\partial f(\nu, V)}{\partial \text{vec}(V)^T} \quad \frac{\partial f(\nu, V)}{\partial \nu} \right]^T \Big|_{(\nu^*, V^*)} = 0. \quad (53)$$

Using the notation of Magnus and Neudecker [40], the derivative of the objective function with respect to $\text{vec}(V)$ is

$$\frac{\partial f(\nu, V)}{\partial \text{vec}(V)} = \frac{\nu - d - 1}{2} \frac{\partial \ln(|V|)}{\partial \text{vec}(V)} - \frac{1}{2} \frac{\partial \text{tr}(V \mathbb{E}[X^{-1}])}{\partial \text{vec}(V)}, \quad (54a)$$

$$= \frac{\nu - d - 1}{2} \text{vec}(V^{-1}) - \frac{1}{2} \text{vec}(\mathbb{E}[X^{-1}]). \quad (54b)$$

Setting (54b) to zero and using Lemma 3:

$$V^* = \left(\frac{\nu^* - d - 1}{\nu^* - d - 1} \right) C_1^{-1}, \quad (55)$$

which is the desired result (48). Similarly, the derivative of the objective function with respect to ν is:

$$\frac{\partial f(\nu, V)}{\partial \nu} = \frac{1}{2} (\ln(|V|) - d \ln(2) - \mathbb{E}[\ln(|X|)]) - \frac{\partial}{\partial \nu} \ln \left(\Gamma_d \left(\frac{\nu - d - 1}{2} \right) \right), \quad (56)$$

which, through the use of Lemma 4 and [23, Theorem 1.4.1] is equivalent to

$$\frac{\partial f(\nu, V)}{\partial \nu} = \frac{1}{2} \left(\ln(|V|) + \sum_{i=1}^d \psi_0 \left(\frac{\nu-d-i}{2} \right) - \sum_{i=1}^d \psi_0 \left(\frac{\nu-d-i}{2} \right) - C_3 \right). \quad (57)$$

Substitution of (55) into (57) and solving for zero yields (49).

To complete the proof, we must now show that the objective function is concave, and that (ν^*, V^*) is the unique global maximum. For the objective function to be concave, the hessian matrix, denoted by $\nabla^2 f(\nu, V)$, must be symmetric negative definite, or conversely $-\nabla^2 f(\nu, V) \in \mathbb{S}_{++}^{(d^2+1)}$, where

$$\nabla^2 f(\nu, V) = \begin{bmatrix} \frac{\partial^2 f(\nu, V)}{\partial \text{vec}(V) \partial \text{vec}(V)^T} & \frac{\partial^2 f(\nu, V)}{\partial \text{vec}(V) \partial \nu} \\ \frac{\partial^2 f(\nu, V)}{\partial \nu \partial \text{vec}(V)^T} & \frac{\partial^2 f(\nu, V)}{\partial \nu \partial \nu} \end{bmatrix}. \quad (58)$$

Using equations (54b), (57) and [41, Section 8.4], the negative of the hessian matrix is equal to

$$-\nabla^2 f(\nu, V) = \begin{bmatrix} \frac{(V^{-1} \otimes V^{-1})}{2(\nu-d-1)^{-1}} & -\frac{1}{2} \text{vec}(V^{-1}) \\ -\frac{1}{2} \text{vec}(V^{-1})^T & \frac{1}{4} \sum_{i=1}^d \psi_1 \left(\frac{\nu-d-i}{2} \right) \end{bmatrix}, \quad (59)$$

where the Kronecker product is symmetric positive definite for all $\nu > 2d$ and $V \in \mathbb{S}_{++}^d$. Hence, using the Schur complement⁷, $-\nabla^2 f(\nu, V)$ is symmetric positive definite if and only if

$$\sum_{i=1}^d \psi_1 \left(\frac{\nu-d-i}{2} \right) > \frac{2}{\nu-d-1} \times \text{vec}(V^{-1})^T (V \otimes V) \text{vec}(V^{-1}), \quad (60)$$

which holds true by Corollary 1. Hence, the objective function is concave, and (ν^*, V^*) is the global minimum of the Kullback-Leibler divergence between $p(X)$ and all \mathcal{IW}_d distributions. Moreover, this minimum is unique. \square

Lemma 3. Let $p(X)$ be the probability density function described in (46). Then,

$$\mathbb{E}[X^{-1}] = (\nu-d-1)C_1, \quad (61)$$

where C_1 denotes the expectation

$$C_1 = \int (M_{\mathbf{x}} \bar{V} M_{\mathbf{x}}^T)^{-1} \mathcal{N}(\mathbf{x}|\mathbf{m}, P) d\mathbf{x}. \quad (62)$$

Proof. Let $X = W^{-1}$. By [23, Theorem 3.4.1],

$$\mathbb{E}[W] = \int W p(W) dW, \quad (63a)$$

$$\mathbb{E}[W] = \iint W \mathcal{W}_d(W|v-d-1, (M_{\mathbf{x}} \bar{V} M_{\mathbf{x}}^T)^{-1}) \times \mathcal{N}(\mathbf{x}|\mathbf{m}, P) dW d\mathbf{x}, \quad (63b)$$

$$= \int (\nu-d-1) (M_{\mathbf{x}} \bar{V} M_{\mathbf{x}}^T)^{-1} \mathcal{N}(\mathbf{x}|\mathbf{m}, P) d\mathbf{x}, \quad (63c)$$

⁷We refer the reader to [42] for further details on the Schur complement.

where the last equality is a consequence of [23, Theorem 3.3.15]. Substitution of (62) yields the desired result. \square

Lemma 4. Let $p(X)$ be the probability density function described in (46). Then,

$$\mathbb{E}[\ln(|X|)] = C_3 - d \ln(2) - \sum_{i=1}^d \psi_0 \left(\frac{\nu-d-i}{2} \right), \quad (64)$$

where C_3 denotes the integral

$$C_3 = \int \ln(|M_{\mathbf{x}} \bar{V} M_{\mathbf{x}}^T|) \mathcal{N}(\mathbf{x}|\mathbf{m}, P) d\mathbf{x}. \quad (65)$$

Proof. By the law of the unconscious statistician [43, pg. 274],

$$\mathbb{E}[\ln(|X|)] = \int \ln(|X|) p(X) dX, \quad (66a)$$

$$= \iint \ln(|X|) \mathcal{IW}_d(X|v, M_{\mathbf{x}} \bar{V} M_{\mathbf{x}}^T) \times \mathcal{N}(\mathbf{x}|\mathbf{m}, P) dX d\mathbf{x}. \quad (66b)$$

Thus, in order to prove (64), we must first find an analytical expression for the following intermediate expectation:

$$\mathbb{E}_{\mathcal{IW}}[\ln(|X|)] \triangleq \int \ln(|X|) \mathcal{IW}_d(X|v, M_{\mathbf{x}} \bar{V} M_{\mathbf{x}}^T) dX. \quad (67)$$

Using the moment generating function, (67) is equivalent to the following partial derivative:

$$\mathbb{E}_{\mathcal{IW}}[\ln(|X|)] = \left. \frac{\partial}{\partial s} \mathbb{E}_{\mathcal{IW}}[|X|^s] \right|_{s=0}, \quad (68)$$

where the expectation

$$\mathbb{E}_{\mathcal{IW}}[|X|^s] = \int |X|^s \mathcal{IW}_d(X|v, M_{\mathbf{x}} \bar{V} M_{\mathbf{x}}^T) dX, \quad (69a)$$

$$= \frac{\Gamma_d \left(\frac{\nu-2s-d-1}{2} \right) |M_{\mathbf{x}} \bar{V} M_{\mathbf{x}}^T|^s}{\Gamma_d \left(\frac{\nu-d-1}{2} \right) 2^{ds}}. \quad (69b)$$

Substituting (69b) into (68), and using Lemmata 7 and 8:

$$\mathbb{E}_{\mathcal{IW}}[\ln(|X|)] = \ln \left(\frac{|M_{\mathbf{x}} \bar{V} M_{\mathbf{x}}^T|}{2^d} \right) - \sum_{i=1}^d \psi_0 \left(\frac{\nu-d-i}{2} \right). \quad (70)$$

Substitution of (70) into (66b) yields (64). \square

Lemma 5. Let $V \in \mathbb{S}_{++}^d$ where $d \in \mathbb{N}$. Then,

$$\text{vec}(V^{-1})^T (V \otimes V) \text{vec}(V^{-1}) = d. \quad (71)$$

Proof. From [23, Theorem 1.2.22]

$$\text{vec}(V^{-1})^T (V \otimes V) \text{vec}(V^{-1}) = \text{vec}(V^{-1})^T \text{vec}(V). \quad (72)$$

Moreover, by [23, Theorem 1.2.10], there exists an orthogonal matrix $H_1 \in \mathbb{O}^{d \times d}$ and diagonal matrix $\Lambda = \text{diag}(\lambda_1, \dots, \lambda_d)$ such that $V = H_1 \Lambda H_1^T$. Therefore,

$$\text{vec}(V^{-1})^T \text{vec}(V) = \text{vec}(H_1 \Lambda^{-1} H_1^T)^T \text{vec}(H_1 \Lambda H_1^T), \quad (73a)$$

$$= \text{vec}(\Lambda^{-1})^T (I_d \otimes I_d) \text{vec}(\Lambda), \quad (73b)$$

$$= \sum_{i=1}^d \frac{1}{\lambda_i} \lambda_i \quad (73c)$$

$$= d. \quad (73d)$$

Substitution of (73d) into (72) yields (71). \square

Lemma 6. Let $\nu > 2d$ where $d \in \mathbb{N}$. Then,

$$\sum_{i=1}^d \psi_1\left(\frac{\nu-d-i}{2}\right) > \frac{2d}{\nu-d-1}. \quad (74)$$

Proof. Consider the following upper bound:

$$\sum_{i=1}^d \frac{2}{\nu-d-i} > \frac{2d}{\nu-d-1}. \quad (75)$$

Thus, rather than solving (74) directly, it suffices to prove

$$\sum_{i=1}^d \left(\psi_1\left(\frac{\nu-d-i}{2}\right) - \frac{2}{\nu-d-i} \right) > 0. \quad (76)$$

A sufficient condition for the inequality to hold is for the difference within the summation to remain positive. That is, for the inequality

$$\psi_1(a_i) - \frac{1}{a_i} > 0 \quad (77)$$

to hold true for all $a_i = \frac{1}{2}(\nu-d-i)$, where $i = 1, \dots, d$. By substitution of recurrence relation $\psi_1(a_i+1) = \psi_1(a_i) - a_i^{-2}$ into [44, Lemma 10],

$$\psi_1(a_i) > \frac{1}{a_i^2} + \frac{2a_i+1}{2a_i^2+2a_i+\frac{2}{3}} > \frac{1}{a_i}, \quad \forall a_i > 0. \quad (78)$$

Hence, inequality (77) holds for all $\nu > 2d$. \square

Corollary 1. Let $V \in \mathbb{S}_{++}^d$ and $\nu > 2d$ where $d \in \mathbb{N}$. Then,

$$\sum_{i=1}^d \psi_1\left(\frac{\nu-d-i}{2}\right) > \frac{2}{\nu-d-1} \times \text{vec}(V^{-1})^T (V \otimes V) \text{vec}(V^{-1}). \quad (79)$$

Proof. Substitute Lemma 5 into Lemma 6. \square

Lemma 7. Let the scalar $\nu > 2s + 2d$, where $s \in \mathbb{R}$ and $d \in \mathbb{N}$. Then,

$$\begin{aligned} \frac{\partial}{\partial s} \Gamma_d\left(\frac{\nu-2s-d-1}{2}\right) &= -\Gamma_d\left(\frac{\nu-2s-d-1}{2}\right) \\ &\times \sum_{i=1}^d \psi_0\left(\frac{\nu-2s-d-i}{2}\right). \end{aligned} \quad (80)$$

Proof. In accordance with logarithmic differentiation,

$$\begin{aligned} \frac{\partial}{\partial s} \Gamma_d\left(\frac{\nu-2s-d-1}{2}\right) &= \Gamma_d\left(\frac{\nu-2s-d-1}{2}\right) \\ &\times \frac{\partial}{\partial s} \ln\left(\Gamma_d\left(\frac{\nu-2s-d-1}{2}\right)\right), \end{aligned} \quad (81)$$

where, via [23, Theorem 1.4.1],

$$\begin{aligned} \frac{\partial}{\partial s} \ln\left(\Gamma_d\left(\frac{\nu-2s-d-1}{2}\right)\right) &= \frac{\partial}{\partial s} \frac{d(d-1)}{4} \ln(\pi) + \\ &\sum_{i=1}^d \frac{\partial}{\partial s} \ln\left(\Gamma\left(\frac{\nu-2s-d-i}{2}\right)\right), \end{aligned} \quad (82a)$$

$$= -\sum_{i=1}^d \psi_0\left(\frac{\nu-2s-d-i}{2}\right). \quad (82b)$$

Substitution of (82b) into (81) yields (80). \square

Lemma 8. Let $s \in \mathbb{R}$, and $V \in \mathbb{S}_{++}^d$ where $d \in \mathbb{N}$. Then,

$$\frac{\partial}{\partial s} \frac{|M_{\mathbf{x}} \bar{V} M_{\mathbf{x}}^T|^s}{2^{ds}} = \ln\left(\frac{|M_{\mathbf{x}} \bar{V} M_{\mathbf{x}}^T|}{2^d}\right) \frac{|M_{\mathbf{x}} \bar{V} M_{\mathbf{x}}^T|^s}{2^{ds}} \quad (83)$$

Proof. Given $a^s = \exp(s \ln(a))$,

$$\frac{\partial}{\partial s} \frac{|M_{\mathbf{x}} \bar{V} M_{\mathbf{x}}^T|^s}{2^{ds}} = \frac{\partial}{\partial s} \exp\left(s \ln\left(\frac{|M_{\mathbf{x}} \bar{V} M_{\mathbf{x}}^T|}{2^d}\right)\right), \quad (84a)$$

$$= \ln\left(\frac{|M_{\mathbf{x}} \bar{V} M_{\mathbf{x}}^T|}{2^d}\right) \frac{|M_{\mathbf{x}} \bar{V} M_{\mathbf{x}}^T|^s}{2^{ds}}. \quad (84b)$$

\square

Lemma 9. Let the state transition degrees of freedom v_{k+1} be defined by (35). Then,

$$\begin{aligned} \text{Vol}(\mathbb{E}[X_{k+1}|\mathbf{Z}^k]) &= \\ \text{Vol}\left(\int M_{\mathbf{x}_k} \mathbb{E}[X_k|\mathbf{Z}^k] H M_{\mathbf{x}_k}^T \mathcal{N}(\mathbf{x}_k|\mathbf{m}_{k|k}, P_{k|k}) d\mathbf{x}_k\right), \end{aligned} \quad (85)$$

where $H = (I_d + Q_{k+1} V_{k|k})^{-1} |I_d + Q_{k+1} V_{k|k}|^{\frac{1}{d}} \in \mathbb{S}\mathbb{L}(d, \mathbb{R})$.

Proof. Let $\bar{\mathbb{E}}[X_{k+1}|\mathbf{Z}^k]$ denote the expected value of (26a). In accordance with [23, Theorem 3.4.3]

$$\bar{\mathbb{E}}[X_{k+1}|\mathbf{Z}^k] = \int \frac{M_{\mathbf{x}_k} \bar{V}_{k+1} M_{\mathbf{x}_k}^T}{v_{k+1} - 2d - 2} \mathcal{N}(\mathbf{x}_k|\mathbf{m}_{k|k}, P_{k|k}) d\mathbf{x}_k. \quad (86)$$

However, from (26b) and (35),

$$\frac{\bar{V}_{k+1}}{v_{k+1} - 2d - 2} = \frac{V_{k|k} (I_d + Q_{k+1} V_{k|k})^{-1}}{(v_{k|k} - 2d - 2) |I_d + Q_{k+1} V_{k|k}|^{-\frac{1}{d}}}, \quad (87a)$$

$$= \mathbb{E}[X_k|\mathbf{Z}^k] \frac{(I_d + Q_{k+1} V_{k|k})^{-1}}{|I_d + Q_{k+1} V_{k|k}|^{-\frac{1}{d}}}. \quad (87b)$$

Substituting (87b) into (86) and defining the special linear group matrix $H = (I_d + Q_{k+1} V_{k|k})^{-1} |I_d + Q_{k+1} V_{k|k}|^{\frac{1}{d}}$, the expected value becomes:

$$\begin{aligned} \bar{\mathbb{E}}[X_{k+1}|\mathbf{Z}^k] &= \int M_{\mathbf{x}_k} \mathbb{E}[X_k|\mathbf{Z}^k] H M_{\mathbf{x}_k}^T \\ &\times \mathcal{N}(\mathbf{x}_k|\mathbf{m}_{k|k}, P_{k|k}) d\mathbf{x}_k. \end{aligned} \quad (88)$$

Finally, from Theorem 1, the following equality holds true:

$$\text{Vol}(\mathbb{E}[X_{k+1}|\mathbf{Z}^k]) = \text{Vol}(\bar{\mathbb{E}}[X_{k+1}|\mathbf{Z}^k]). \quad (89)$$

Substitution of (88) into (89) yields (85). \square

REFERENCES

- [1] Y. Bar-Shalom, *Tracking and data association*. Academic Press Professional, Inc., 1987.
- [2] K. Gilholm and D. Salmund, "Spatial distribution model for tracking extended objects," *IEE Proceedings-Radar, Sonar and Navigation*, vol. 152, no. 5, pp. 364–371, 2005.
- [3] Y. Boers, H. Driessen, J. Torstensson, M. Trieb, R. Karlsson, and F. Gustafsson, "Track-before-detect algorithm for tracking extended targets," *IEE Proceedings-Radar, Sonar and Navigation*, vol. 153, no. 4, pp. 345–351, 2006.
- [4] D. Angelova, L. Mihaylova, N. Petrov, and A. Gning, "A convolution particle filtering approach for tracking elliptical extended objects," in *Proceedings of the 16th International Conference on Information Fusion*. IEEE, 2013, pp. 1542–1549.
- [5] R. Mahler, "PHD filters for nonstandard targets, I: Extended targets," *2009 12th International Conference on Information Fusion*, no. July 2009, pp. 448–452, 2009.

- [6] M. Baum and U. D. Hanebeck, "Random hypersurface models for extended object tracking," in *2009 IEEE International Symposium on Signal Processing and Information Technology (ISSPIT)*. IEEE, 2009, pp. 178–183.
- [7] C. Lundquist, K. Granström, and U. Orguner, "Estimating the Shape of Targets with a PHD Filter," in *14th International Conference on Information Fusion*, 2011, pp. 1–8.
- [8] T. Hirscher, A. Scheel, S. Reuter, and K. Dietmayer, "Multiple extended object tracking using Gaussian processes," in *2016 19th International Conference on Information Fusion (FUSION)*, IEEE. ISIF, 2016, pp. 868–875.
- [9] S. Yang and M. Baum, "Tracking the orientation and axes lengths of an elliptical extended object," *IEEE Transactions on Signal Processing*, vol. 67, no. 18, pp. 4720–4729, 2019.
- [10] J. W. Koch, "Bayesian approach to extended object and cluster tracking using random matrices," *IEEE Transactions on Aerospace and Electronic Systems*, vol. 44, no. 3, 2008.
- [11] M. Feldmann, D. Franken, and W. Koch, "Tracking of extended objects and group targets using random matrices," *IEEE Transactions on Signal Processing*, vol. 59, no. 4, pp. 1409–1420, 2011.
- [12] J. Lan and X. R. Li, "Tracking of extended object or target group using random matrix: new model and approach," *IEEE Transactions on Aerospace and Electronic Systems*, vol. 52, no. 6, pp. 2973–2989, 2016.
- [13] K. Granström and U. Orguner, "A new prediction for extended targets with random matrices," *IEEE Transactions on Aerospace and Electronic Systems*, vol. 50, no. 2, pp. 1577–1589, 2014.
- [14] N. J. Bartlett, C. Renton, and A. G. Wills, "A Closed-Form Prediction Update for Extended Target Tracking using Random Matrices," *IEEE Transactions on Signal Processing*, vol. 68, pp. 2404–2418, 2020.
- [15] K. Granström and U. Orguner, "A PHD filter for tracking multiple extended targets using random matrices," *IEEE Transactions on Signal Processing*, vol. 60, no. 11, pp. 5657–5671, 2012.
- [16] K. Granström, A. Natale, P. Braca, G. Ludeno, and F. Serafino, "Gamma Gaussian inverse Wishart probability hypothesis density for extended target tracking using X-band marine radar data," *IEEE Transactions on Geoscience and Remote Sensing*, vol. 53, no. 12, pp. 6617–6631, 2015.
- [17] K. Granström, M. Baum, and S. Reuter, "Extended Object Tracking: Introduction, Overview and Applications," *Journal of Advances in Information Fusion (JAIF)*, vol. 12, no. 2, pp. 139–174, 2017.
- [18] K. Granström, S. Renter, M. Fatemi, and L. Svensson, "Pedestrian tracking using Velodyne data-Stochastic optimization for extended object tracking," *2017 IEEE Intelligent Vehicles Symposium*, no. IV, pp. 39–46, 2017.
- [19] G. Vivone, P. Braca, K. Granström, A. Natale, and J. Chanussot, "Converted measurements random matrix approach to extended target tracking using X-band marine radar data," in *2015 18th International Conference on Information Fusion (Fusion)*. IEEE, 2015, pp. 976–983.
- [20] —, "Converted measurements Bayesian extended target tracking applied to x-band marine radar data," *Journal of Advances in Information Fusion*, vol. 12, no. 2, pp. 189–210, 2019.
- [21] M. Schuster, J. Reuter, and G. Wanielik, "Probabilistic data association for tracking extended targets under clutter using random matrices," in *2015 18th International Conference on Information Fusion (Fusion)*. IEEE, 2015, pp. 961–968.
- [22] M. Beard, S. Reuter, K. Granström, B.-T. Vo, B.-N. Vo, and A. Scheel, "Multiple Extended Target Tracking With Labeled Random Finite Sets," *IEEE Transactions on Signal Processing*, vol. 64, no. 7, pp. 1638–1653, 2016.
- [23] A. K. Gupta and D. K. Nagar, *Matrix variate distributions*. Chapman & Hall/CRC, London, 2000, vol. 104.
- [24] M. Feldmann and D. Franken, "Tracking of extended objects and group targets using random matrices—a new approach," in *2008 11th International Conference on Information Fusion*. IEEE, 2008, pp. 1–8.
- [25] J. Lan and X. R. Li, "Tracking of extended object or target group using random matrix - Part I: New model and approach," in *2012 15th International Conference on Information Fusion*. IEEE, 2012, pp. 2177–2184.
- [26] K. Granström and U. Orguner, *Properties and approximations of some matrix variate probability density functions*. Linköping University Electronic Press, 2011.
- [27] K. Granström and J. Bramstång, "Bayesian Smoothing for the Extended Object Random Matrix Model," *IEEE Transactions on Signal Processing*, vol. 67, no. 14, pp. 3732–3742, 2019.
- [28] R. Mahler, *Statistical Multisource-Multitarget Information Fusion*. Artech House, Inc., 2007.
- [29] G. Vivone, K. Granström, P. Braca, and P. Willett, "Multiple sensor Bayesian extended target tracking fusion approaches using random matrices," in *2016 19th International Conference on Information Fusion (FUSION)*, no. July, 2016, pp. 886–892.
- [30] X. R. Li and V. P. Jilkov, "Survey of maneuvering target tracking: Dynamic models," *Signal and Data Processing of Small Targets 2000*, vol. 4048, no. April, pp. 212–235, 2000.
- [31] —, "Survey of Maneuvering Target Tracking. Part I: Dynamic Models," *IEEE Transactions on Aerospace and Electronic Systems*, vol. 39, no. 4, pp. 1333–1364, 2003.
- [32] S. F. Schmidt, "Application of state-space methods to navigation problems," in *Advances in control systems*. Elsevier, 1966, vol. 3, pp. 293–340.
- [33] G. L. Smith, S. F. Schmidt, and L. A. McGee, *Application of statistical filter theory to the optimal estimation of position and velocity on board a circumlunar vehicle*. National Aeronautics and Space Administration, 1962.
- [34] J. L. Williams and P. S. Maybeck, "Cost-function-based Gaussian mixture reduction for target tracking," in *Proceedings of the sixth international conference of information fusion*, vol. 2. IEEE Publ. Piscataway, NJ, 2003, pp. 1047–1054.
- [35] A. R. Runnalls, "Kullback-Leibler approach to Gaussian mixture reduction," *IEEE Transactions on Aerospace and Electronic Systems*, vol. 43, no. 3, pp. 989–999, 2007.
- [36] J. R. Hershey and P. A. Olsen, "Approximating the Kullback Leibler divergence between Gaussian mixture models," in *2007 IEEE International Conference on Acoustics, Speech and Signal Processing-ICASSP'07*, vol. 4. IEEE, 2007, pp. 317–320.
- [37] S. Kullback and R. A. Leibler, "On information and sufficiency," *The annals of mathematical statistics*, vol. 22, no. 1, pp. 79–86, 1951.
- [38] J. M. Ortega and W. C. Rheinboldt, *Iterative solution of nonlinear equations in several variables*. Siam, 1970, vol. 30.
- [39] S. Yang, M. Baum, and K. Granström, "Metrics for performance evaluation of elliptic extended object tracking methods," in *2016 IEEE International Conference on Multisensor Fusion and Integration for Intelligent Systems (MFI)*. IEEE, 2016, pp. 523–528.
- [40] J. R. Magnus and H. Neudecker, "Matrix differential calculus with applications to simple, Hadamard, and Kronecker products," *Journal of Mathematical Psychology*, vol. 29, no. 4, pp. 474–492, 1985.
- [41] —, *Matrix Differential Calculus with Applications in Statistics and Econometrics*, third edit ed. John Wiley & Sons, 1999.
- [42] F. Zhang, *The Schur complement and its applications*. Springer Science & Business Media, 2006, vol. 4.
- [43] P. Billingsley, *Probability and measure*, third edit ed. John Wiley & Sons, New York, 1995.
- [44] Z.-H. Yang, Y.-M. Chu, and X.-J. Tao, "A double inequality for the Trigamma function and its applications," *Abstract and Applied Analysis*, vol. 2014, no. 3, 2014.